International Journal of Hydraulic Engineering 2013, 2(2): 21-27
DOI: 10.5923/j.ijhe.20130202.01

Hydrodynamic Characteristics of Gradually Expanded Channel Flow

Edward Ching-Ruey LUO

Department of Civil Engineering, National Chi-Nan University. 227 Gan-Cherng St. Taichung 40843, Taiwan

Abstract In this study, analytical-statistical solutions of the characteristics in gradually expanded channel flows, such as velocity profile, turbulent shear stress profile and profiles of turbulent kinetic energy, energy dissipation rate, and dispersion coefficient are derived. Then, the comparisons of the analytical results are made with the results of 2-DH with depth-averaged numerical model solution. Good trends and agreements are obtained, and the expanding angle takes an important and relevant role on the main effect of these hydrodynamic items. These analytical-statistical solutions can be used for real applications on water power plant and water quality control.

Keywords Velocity Profile, Turbulent Shear Stress, Turbulent Kinetic Energy, Energy Dissipation Rate, Dispersion, Turbulence, Gradually Expanded Flow, Hydrodynamics, Water Quality, Water Power Plant

1. Introduction

As the direct result of turbulence generates at the boarders of a free or submerged case inlet jet, the fluid within the jet undergoes both lateral diffusion and deceleration, and at the same time, fluid from the surrounding region is brought into motion in more explicit terms. The difference in velocity between a jet and the region into which it is discharged gives rise to a pronounced degree of instability, and the latter steadily decaying through viscous shear forming energy dissipation rate. In view of the Newtonian principle of motion between action and reaction, moreover, it is realized that deceleration of the fluid in the jet can occur only through simultaneously acceleration of the surrounding fluid, so that the total rate of flow passing through successive sections of the jet actually increases with distance from the outlet. In the cases of $\beta=0°$, $0°<\beta<4.6°$, and $\beta\geqq 4.6°$, the circulating flow situation happens from the entrance until certain distance downstream. Within the circulation region, convective term, diffusion term, bottom stress, and the dispersion term in 2-D model exist due to the reason for the depth-integrated method from 3-D flow equation. The new velocity profile must be re-derived, and then the analytical turbulent shear stress, turbulent kinetic energy, and energy dissipation rate profiles are shown respectively for different β situations. After those procedures, the comparisons between numerical and analytical results are done to express the validity and reliability of the analyses.

* Corresponding author:
edward.luo@msa.hinet.net (Edward Ching-Ruey LUO)
Published online at http://journal.sapub.org/ijhe

2. Analytical Results

In Luo[1], the proposed resultant equations are :

1. For $0°<\beta<4.6°$, $p^*=1.105\beta-0.565\beta^2+0.08\beta^3\leqq 0.5$:

A. Primary velocity profile

$$\frac{U(y)}{u_*}=\frac{1}{\kappa}\ln\left(\frac{10yu_*}{\nu}\right)+\frac{K}{2\kappa}\left(\frac{yp^*}{r}\right)\left(\frac{U_0}{u_*}\right)^2 \tag{1}$$

B. Turbulent shear stress profile

$$\frac{\tau_w}{\rho}=u_*^2+\frac{p^*U_0^2y}{4r} \tag{2}$$

C. Turbulent viscosity coefficient

$$\nu_{(ty)}=\frac{(\tau_w/\rho)}{[dU(y)/dy]}=\kappa yu_* \tag{3}$$

D. Turbulent kinetic energy profile

$0<\beta<4.6^o$

$$\bar{k}=\frac{1}{2}\left\{0.027\left(\frac{\nu B_0\bar{U}+\nu h_0U_0}{U_0h_0B_e\bar{U}}\right)^{1/4}U^2+\left(\frac{3p^*U_0^2y}{10r\cos\beta}\right)+\right. \tag{4}$$

$$\left.-\frac{U_0^4y^4p^{*2}\sec^2\beta}{30r^4u_*^2}\right\}$$

E. Energy dissipation rate profile

$$\bar{\varepsilon}=C_\mu\frac{\bar{k}^2}{\bar{\nu}_t} \tag{5}$$

F. Dispersion Coefficient

$$\overline{D}_y = \frac{-1}{B_e}\int_0^{B_e} U'(y)\int_0^{y}\frac{1}{\nu_{ty}}\int_0^{y} U'(y)\,dy\,dy\,dy \tag{6}$$

and

$$U(y) - \overline{U}(y) = U'(y) \tag{7}$$

where $\overline{U}(y)$ is the integration of U(y) with respect to the width B along the flow

$$\overline{D}_y = \frac{u_* B_e}{2\kappa^3} + \frac{0.625 p^* B_e^2 U_0^2}{12\kappa^2 r u_*} - \frac{p^{*2} B_e^3 U_0^4}{123 r^2 u_*^3 \kappa} \tag{8}$$

2. For $\beta \geqq 4.6°$ and $p^* = 0.5$ for $\beta \geqq 4.6°$:

A. Primary velocity profile

$$\frac{U(y)}{u_*} = \frac{2}{\kappa}\left(\frac{y}{l}\right)^{1/2} = \frac{2}{\kappa}\left(\frac{yp^*}{r}\right)^{1/2}\left(\frac{U_0}{u_*}\right)\left(\frac{B_0}{B_e}\right) \tag{9}$$

B. Turbulent shear stress profile

$$\frac{\tau_w}{\rho} = \left(\frac{U_0 u_* B_0}{B_e}\right)\left(\frac{y}{2r}\right)^{\frac{1}{2}} \tag{10}$$

C. Turbulent viscosity coefficient

$$\nu_{(ty)} = \frac{(\tau_w/\rho)}{[dU(y)/dy]} = \kappa y u_* \tag{11}$$

D. Turbulent kinetic energy profile

$$\overline{k} = \frac{1}{2}\left(\overline{u'^2} + \overline{v'^2}\right) = \frac{1}{2\rho}\left(\overline{\tau}_{xx} + \overline{\tau}_{yy}\right)$$

$$= \frac{1}{2}\left\{0.027\left(\frac{\nu B_e \overline{U} + \nu h_0 U_0}{U_0 h_0 \overline{U} B_e}\right)^{1/4} U^2 + \left(\frac{13 U_0 u_* y}{20 r \cos\beta}\right)\left(\frac{B_e}{B_o}\right)^{1/4} + \right. \tag{12}$$

$$\left. - \frac{U_0^2 y^2 B_0^2}{36\kappa^2 r^2 B_e^2}\right\}$$

E. Energy dissipation rate profile

$$\overline{\varepsilon} = C_\mu \frac{\overline{k}^2}{\overline{\nu}_t} \tag{13}$$

F. Dispersion Coefficient

$$\overline{D}_y = \left(\frac{16 B_e^2}{\kappa^3 r}\right)\left(\frac{U_0^2}{u_*}\right)\left(\frac{B_0}{B_e}\right)^2 \tag{14}$$

3. For $\beta = 0°$:

A. Primary velocity profile

$$\frac{U(y)}{u_*} = \frac{1}{\kappa}\ln\left(\frac{10 y u_*}{\nu}\right) \tag{15}$$

B. Turbulent shear stress profile

$$\frac{\tau_w}{\rho} = u_*^2 \tag{16}$$

C. Turbulent viscosity coefficient

$$\nu_{(ty)} = \frac{(\tau_w/\rho)}{[dU(y)/dy]} = \kappa y u_* \tag{17}$$

D. Turbulent kinetic energy profile

$$\beta = 0^o$$

$$\overline{k} = \frac{1}{2}\left\{0.027\left(\frac{\nu B_0 \overline{U} + \nu h_0 U_0}{U_0 h_0 \overline{U} B_0}\right)^{1/4} . U^2\right\} \tag{18}$$

E. Energy dissipation rate profile

$$\overline{\varepsilon} = C_\mu \frac{\overline{k}^2}{\overline{\nu}_t} \tag{19}$$

F. Dispersion Coefficient

$$\overline{D}_y = \frac{0.404}{\kappa^3} B_e u_* \tag{20}$$

3. Comparisons

The 2-DH numerical models are based on the depth averaged equations as follows:

$$\frac{\partial}{\partial x}(HU^2) + \frac{\partial}{\partial y}(HUV) + gH\frac{\partial \xi}{\partial x} + \frac{\tau_{bx}}{\rho} - \frac{\partial(HT_{xx})}{\rho \partial x} - \frac{\partial(HT_{xy})}{\rho \partial y} = 0 \tag{21}$$

$$\frac{\partial(HUV)}{\partial x} + \frac{\partial(HV^2)}{\partial y} + gH\frac{\partial \xi}{\partial y} + \frac{\tau_{by}}{\rho} - \frac{\partial(HT_{xy})}{\rho \partial x} - \frac{\partial(HT_{yy})}{\rho \partial y} = 0 \tag{22}$$

$$T_{xx}^* = \left(-\frac{H}{\rho}\right)T_{xx}; T_{yy}^* = \left(\frac{H}{T}\right)T_{yy};$$

and

$$T_{xy}^* = \left(-\frac{H}{\rho}\right)T_{xy}; \tag{23}$$

And 2-DH k- ε equations:

$$\overline{U}\frac{\partial \overline{k}}{\partial x} + \overline{V}\frac{\partial \overline{k}}{\partial x} = \frac{\partial}{\partial x}\left(\frac{\overline{\nu}_t}{\sigma_k}\frac{\partial \overline{k}}{\partial x}\right) + \frac{\partial}{\partial y}\left(\frac{\overline{\nu}_t}{\sigma_t}\frac{\partial \overline{k}}{\partial y}\right) + P_h + P_{kv} - \varepsilon \tag{24}$$

$$\overline{U}\frac{\partial \overline{\varepsilon}}{\partial x} + \overline{V}\frac{\partial \overline{\varepsilon}}{\partial y} = \frac{\partial}{\partial x}\left(\frac{\overline{\nu}_t}{\sigma_\varepsilon}\frac{\partial \overline{\varepsilon}}{\partial x}\right) + \frac{\partial}{\partial y}\left(\frac{\overline{\nu}_t}{\sigma_\varepsilon}\frac{\partial \overline{\varepsilon}}{\partial y}\right) + C_{1\varepsilon}\left(\frac{\overline{\varepsilon}}{\overline{k}}\right)P_h + P_{\varepsilon v} - C_{2\varepsilon}\left(\frac{\overline{\varepsilon}^2}{\overline{k}}\right) \tag{25}$$

$$P_h = \overline{\nu}_t\left[2\left(\frac{\partial \overline{U}}{\partial x}\right)^2 + 2\left(\frac{\partial \overline{V}}{\partial y}\right)^2 + \left(\frac{\partial \overline{U}}{\partial y} + \frac{\partial \overline{V}}{\partial x}\right)^2\right] \tag{26}$$

$$P_{kv} = C_k\left(\frac{u_*^3}{h}\right); \quad P_{\varepsilon v} = C_\varepsilon\left(\frac{u_*^4}{h^2}\right) \tag{27}$$

$$u_*^2 = C_f\left(\overline{U}^2 + \overline{V}^2\right) \tag{28}$$

$$C_K = \frac{1}{\sqrt{C_f}}; \quad C_\varepsilon = \frac{3.6 C_{2\varepsilon}}{C_f^{3/2}}\sqrt{C_\mu} \tag{29}$$

$$C_f = \frac{n^2 g}{h^{1/3}} \tag{30}$$

Based on Rodi[2] suggested , in near-wall region, a logarithmic velocity profile with neglecting the prevails

fluctuating pressure the 2-DH k- ε can be reduced to:

$$C_{1\varepsilon} = C_{2\varepsilon} - \frac{\kappa^2}{\sigma\sqrt{C_\mu}} \tag{31}$$

The values recommended by Launder and Spalding[3] on Eq. (25) are as follows:

$C_\mu = 0.09$; $C_{1\varepsilon} = 1.44$; $C_{2\varepsilon} = 1.92$; $\sigma_k = 1.0$; $\sigma_\varepsilon = 1.3$ (32)

The 2-DH gradually expanded flow numerical scheme with different angel of β, such as Yu et al[4] and Gayathri S. et al. [5], is in Fig.1, and the comparisons between numerical and analytical results are following in Figs. 2, 3, and 4, respectively.

4. Conclusions and Application

1. The analytical primary velocity profiles, profiles of turbulent kinetic energy and energy dissipation rate for two dimensional horizontal plane diffuser-wall flows outside of the turbulent boundary layers are compared with the corresponding situations from the numerical results. It can be seen from Fig. 2 that the uniform velocity at inlet of 0.5 m/s decreases as it moves downstream. These velocity profiles at x =0.5, 1.0, 1.5, and 2.0 m are in Fig. 3 together with k and ε, which shows that k and ε decrease as x increase but at slower rate than U. The turbulent kinetic energy shows the smallest reduction from upstream to downstream. These are due to the jet flux and the increasing of turbulent boundary thickness along the flow, respectively. The more uniform decreasing on velocity along the flow to the downstream for a given divergent channel makes the flow better stable even with a little bit decreasing with k and ε, this regulation will give good flow control before the flow goes into power plant in order to avoid the damage on the instruments.

2. The comparisons of analytical and numerical results about velocity, turbulent kinetic energy and energy dissipation rate for different β-value at the position of x =2.0 m from the inlet are shown in Fig. 4. From this figure in the case of $\beta = 3°$, the differences between analytical and numerical results on the velocity profile and two turbulent items are very limited. When $\beta = 6°$, which is located in the region of transition zone of diffuser-wall flows from small core-angel to big one, the comparisons of primary velocity profile, turbulent kinetic energy and energy dissipation rate between analytical and numerical results give a little smaller values than the ones for $\beta = 3°$, but the trends and the agreements are still agreeable and acceptable.

3. In the case of big core-angel diffuser-wall flow, such as $\beta = 30°$ or $\beta = 60°$, which show higher values of k and ε than the results of $\beta = 3°$ and $\beta = 6°$ shown. From Fig. 3, the analytical results of primary velocity and the two turbulent items are larger than the numerical ones at the positions near the inlet, such as x =0.5m. This is due to the different distribution forms of primary velocity, the parabolic distribution for analytical result while logarithmic formula for the numerical one. The logarithmic distribution has higher turbulence and energy loss near to the wall, therefore, the higher turbulent kinetic energy and energy dissipation rate with larger primary velocity are presented near wall, too. And the parabolic form for analytical solutions just express the inverse phenomena.

4. When$\beta<0°$, the dispersion coefficient can be expressed as the following equation, Eq.(33), and after the comparisons of the magnitude of turbulent viscosity and dispersion coefficients with different β-value for different relative width, the results are obtained as Eqs. (34) and (35), then the relative scales of mean dispersions coefficients are presented in Fig. 5.

$$\overline{D}_y = -\frac{1}{B_e}\int_0^{B_e} D_y dy \text{ , that is,}$$

$$\overline{D}_y = \left(\frac{\beta^2 u_* B_e}{2\kappa^3}\right)\left[\frac{\left(\frac{1}{\kappa}\frac{U_c}{u_*} - 5.208\right)^2}{\left(27.12 + \frac{\beta^2}{\kappa^4}\right)}\right] - \left(\frac{\beta^3 u_* B_e}{8\kappa^3}\right)\left[\frac{\left(\frac{1}{\kappa}\frac{U_c}{u_*} - 5.208\right)^3}{\left(27.12 + \frac{\beta^2}{\kappa^4}\right)}\right] +$$

$$+\left(\frac{\beta u_* B_e}{\kappa^3}\right)(\ln B_e)^2\left[\frac{\left(\frac{1}{\kappa}\frac{U_c}{u_*} - 5.208\right)}{\left(27.12 + \frac{\beta^2}{\kappa^4}\right)}\right] + \left(\frac{\beta u_* B_e}{\kappa^3}\right)\left[\frac{\left(\frac{1}{\kappa}\frac{U_c}{u_*} - 5.208\right)^2}{\left(27.12 + \frac{\beta^2}{\kappa^4}\right)}\right](\ln B_e) + \tag{33}$$

$$-\left(\frac{2\beta^2 u_* B_e}{\kappa^3}\right)\left(1 - \frac{1}{2}\ln B_e\right)\left[\frac{\left(\frac{1}{\kappa}\frac{U_c}{u_*} - 5.208\right)^2}{\left(27.12 + \frac{\beta^2}{\kappa^4}\right)}\right]$$

$$\overline{\nu}_{t,\beta<0,} \le \overline{\nu}_{t,\beta=0,} \le \overline{\nu}_{t,0<\beta<4.6^o} \le \overline{\nu}_{t,\beta\ge4.6^o} \tag{34}$$

$$\overline{D}_{\beta<0,} \le \overline{D}_{\beta=0,} \le \overline{D}_{0<\beta<4.6^o} \le \overline{D}_{\beta\ge4.6^o} \tag{35}$$

5. With the following expressing equations for energy loss coefficient, kL, on the situation of gradually expanded flow,

$$k_L = \frac{E_0 - E}{\left(\frac{U_0^2}{2g}\right)} = \left(1 - \frac{A_0}{A}\right)^2$$

$$E_0 = \frac{U_0^2}{2g} + h_0; \quad E = \frac{\overline{U}^2}{2g} + h; \tag{36}$$

$$h = \frac{U_0 h_0}{\overline{U}}$$

and the analytical result of kL is compared with the result from Gerhart, et al[6] in Fig. 6. Good trends are obtained.

From the trends of turbulent kinetic energy and energy dissipation rate of Fig. 4, it is found that these two turbulent items will increase significantly with increasing the half-angel, β. These are because of the phenomena of the jet flux, which reduces the primary velocity and increases the velocity fluctuation at the same time, and the increasing of turbulent boundary layer thickness, which has much more strong eddies with larger energy loss. Generally speaking, the analytical results based on the plane turbulent free jets

for diffuser-wall flows can be valid for wide range of β-value, such as from β=3° to β=60°. The transfer due to diffusion or dispersion phenomena from Yang C. S. et al[7] can be study and discuss further and compare with the diffusion or dispersion coefficients for different divergent angels of this research. Here, in Fig. 6, of 2β =180°, the k_L is between 1.0 and 1.1, and this result has good match one with that of abruptly expanded flow situations on radius or width ratio equal to zero, which means β=90°, in Fig. 7.

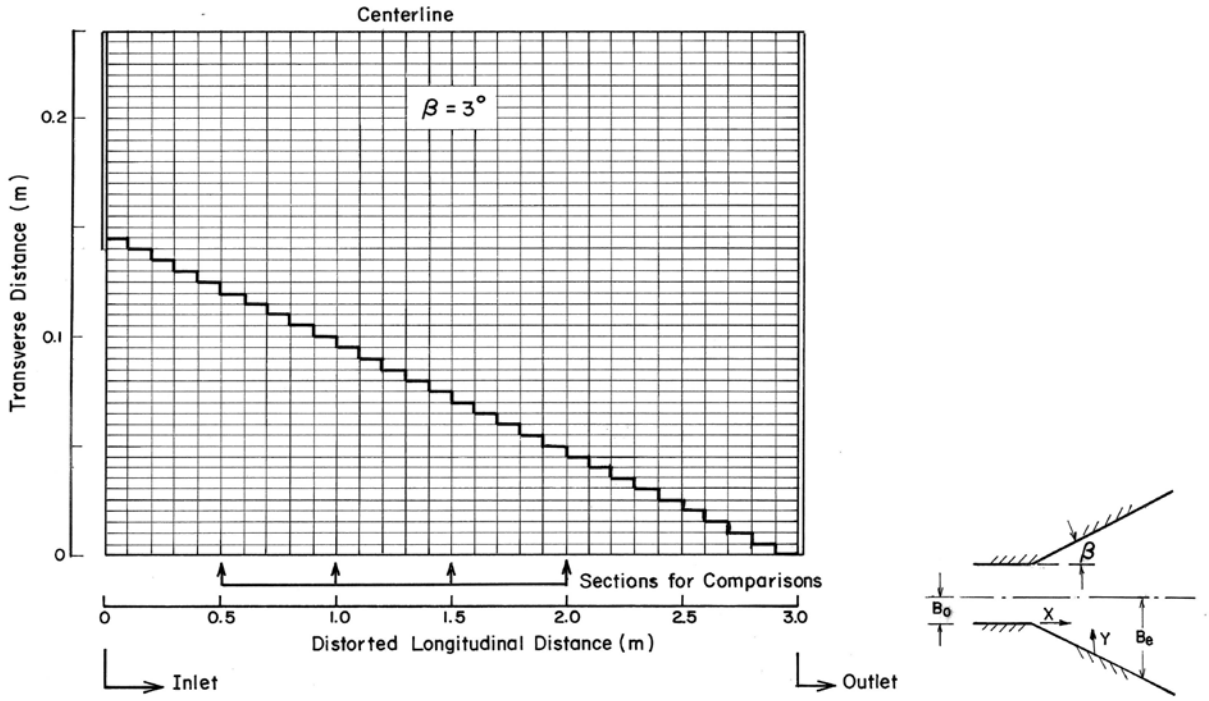

Figure 1. Grid system used in two dimensional depth-averaged model of β=3° with L=3m, Δx=0.1m, Δy=0.01m, Δt=0.06 sec

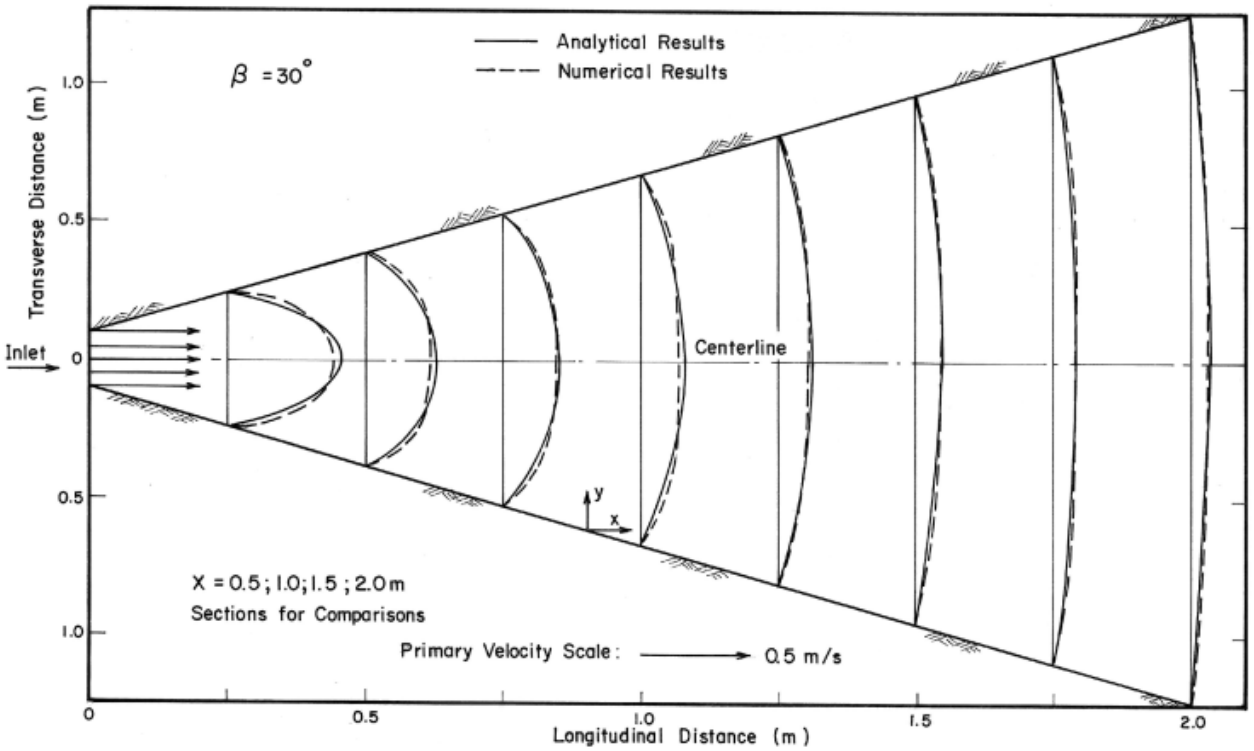

Figure 2. Comparisons of analytical and numerical primary velocity profiles for β=30°, U0=0.5m/s, h0=0.15m, and B0=0.10m

The energy dissipation rate, ε, in Fig. 4, has the consistency with the trend of Fig. 6, on energy loss coefficient, and this shows us again that flow regulation with divergent channel can effectively reach flow uniformity with reduction of the turbulence in main flow direction for mitigation on the damage risk of power plant. We also can get some good information from Eqs. (34) and (35), for both turbulent viscosity for sedimentation and dispersion coefficient for contamination. These parameters express the significant efficiencies on solid particles spreading or settlement on the width direction to protect the turbines.

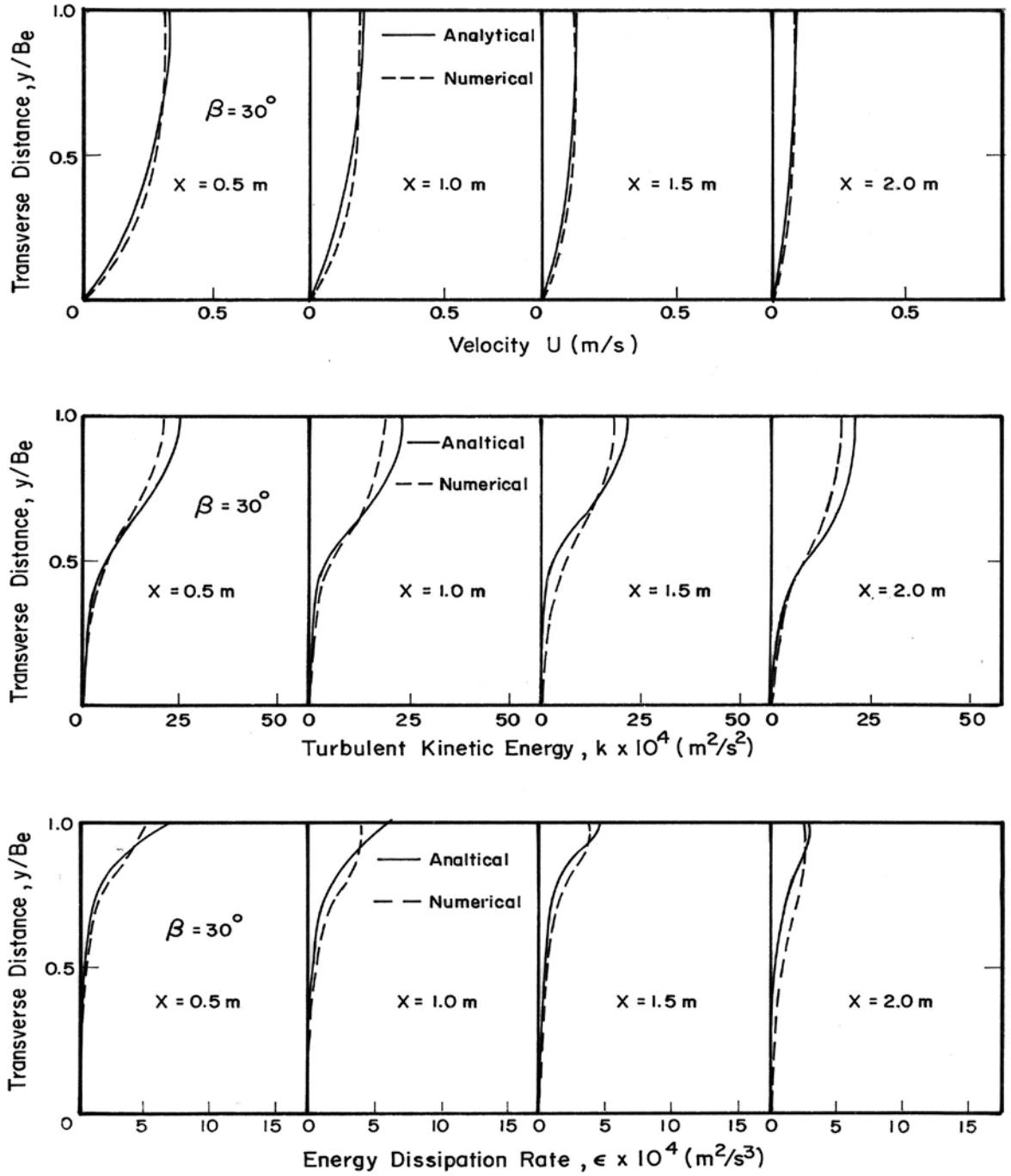

Figure 3. Comparisons of primary velocity U, turbulent kinetic energy k, and energy dissipation rate ε, between analytical and numerical results for diffuser- wall flow with β＝30°, ν＝0.001m2/s, U0=0.5m/s, h0＝0.15m, and B0＝0.10m.along the primary flow direction

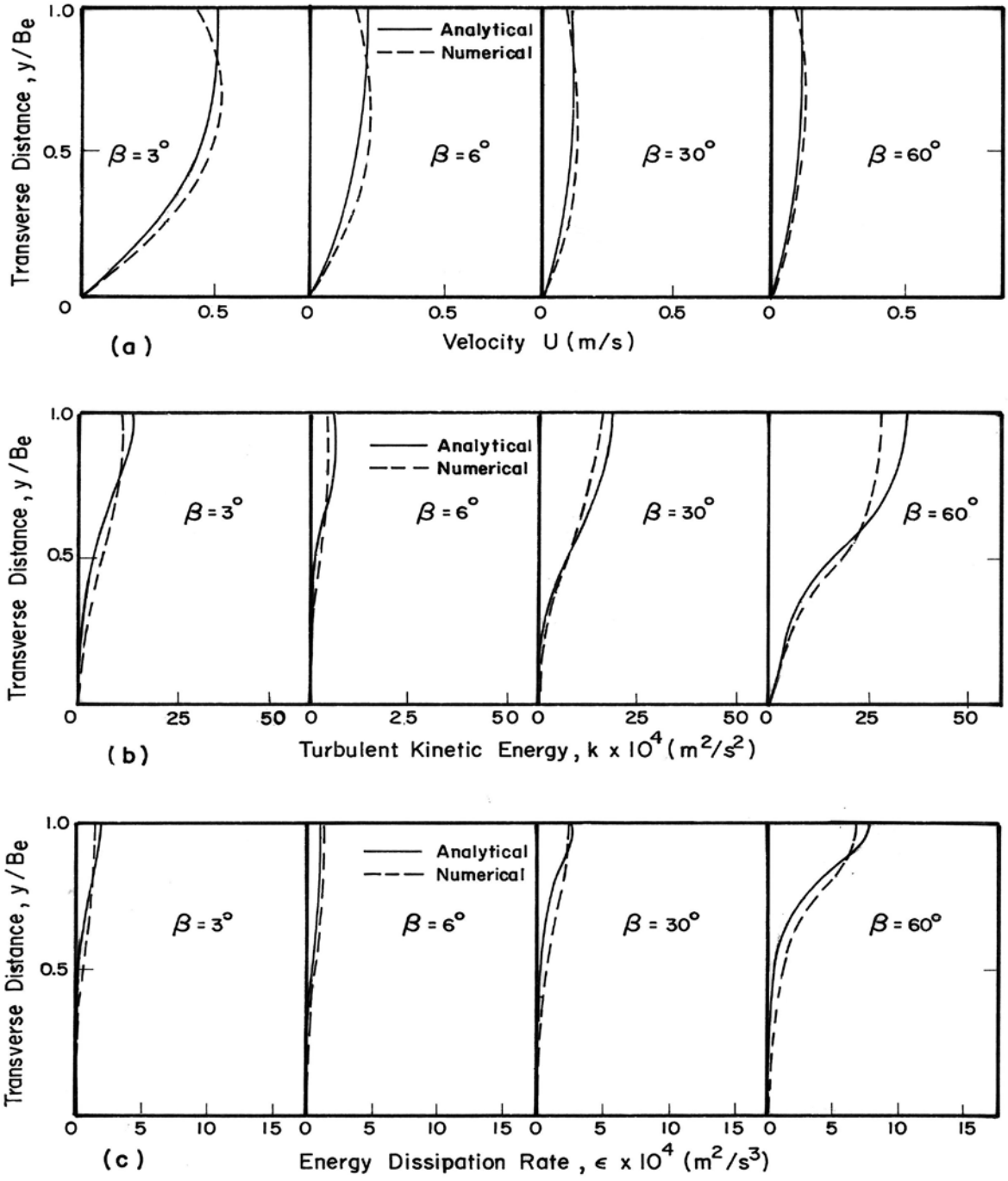

Figure 4. Comparisons of primary velocity U, turbulent kinetic energy k, and energy dissipation rate ε, between analytical and numerical results for different diffuser- wall β- value flow with ν=0.001m2/s, U0=0.5m/s, h0=0.15m, B0=0.10m, and X=2m .along the primary flow direction

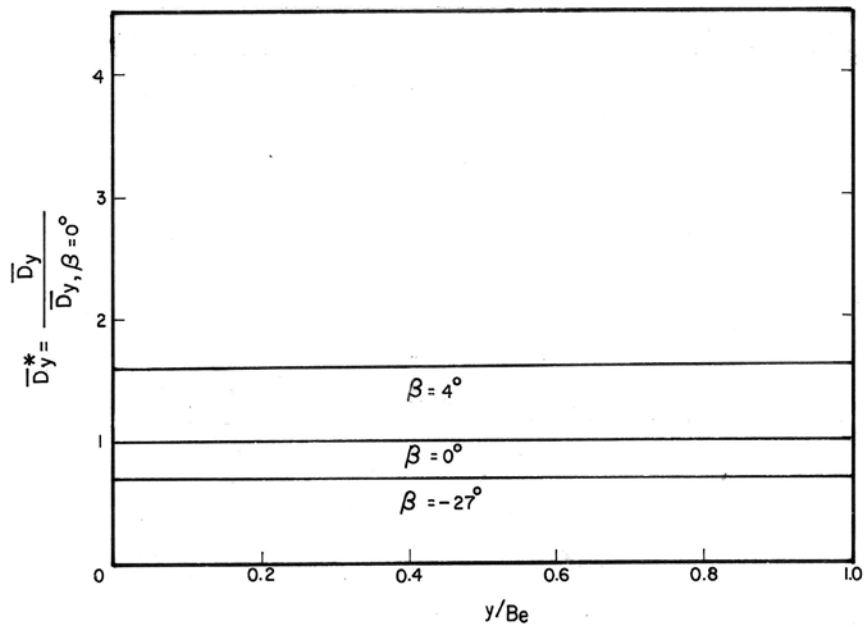

Figure 5. Distributions of dimensionless dispersion coefficients value outside boundary for differentβ-value with B0＝5m, X＝10m, U0＝0.7m/s, friction velocity 0.050m/s, κ＝0.4, and h＝0.15m

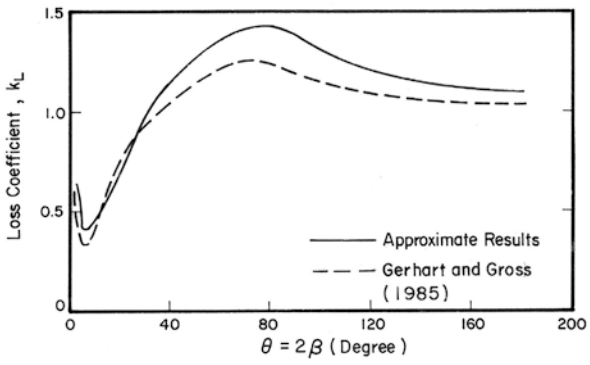

Figure 6. Comparison of energy loss coefficient, KL, for gradually divergent wall flow between approximate results and experimental ones from Gerhart, et al (1985)

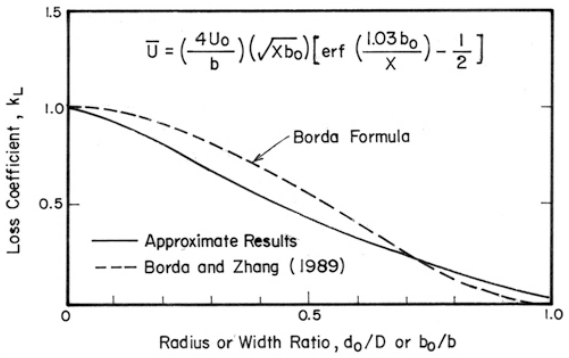

Figure 7. Comparison of energy loss coefficient, KL, for Abruptly expanded channel flow between approximate results and experimental ones from Gerhart, et al (1985)

REFERENCES

[1] C. R. Luo,"Hydrodynamic characteristics in non-uniform channels". Dissertation No.WA 93-1, Asian Institute of Technology, Thailand, 1993.

[2] W. Rodi, " Turbulence models and their application " 1980.

[3] B. E. Launder, and D. B. Spalding, "Mathematical model of turbulence" Dept. of Mechanical Eng. Imperial College of Science and Technology, London, England, 1974.

[4] Yu Z. S.et al., "Numerical computations of flow in a finite diverging channel" J. of Zhejiang Univ-Sci A (Appl Phys & Eng) 2011 11(1).

[5] Gayathri S. et al.," Global instabilities in diverging channel flows " Theoretical and computational fluid dynamics Vol.25. No. 1-4 pp. 53-64, 2011.

[6] Gerhart, P.G. and Gross, R. J., "Fundamentals of fluid mechanics". Addison-Wesley Publishing Company, Inc., Canada, 1985.

[7] Yang C. S. et al.,"Fluid flow and heat transfer in a horizontal channel with divergent top wall and heat from below ".J. of Heat transfer Vol.132, Issue 8, 2010.